

## IMPACT OF RF AND DC PLASMA ON WOOD STRUCTURE\*

A. AVRAM<sup>1,2</sup>, V. COVLEA<sup>3</sup>, A. MATEI<sup>1</sup>, M. BAZAVAN<sup>3</sup>, B. BUTOI<sup>3</sup>, B. BITA<sup>1,3</sup>, E. BARNA<sup>3</sup>  
and A. JIPA<sup>3</sup>

<sup>1</sup>National Institute for R&D in Microtechnologies, 126A Erou Iancu Nicolae street, 023573,  
Bucharest, Romania, E-mail: andrei.avram@imt.ro

<sup>2</sup>University “Politehnica” of Bucharest, Faculty of Electrical Engineering, 313 Splaiul Independentei,  
060042, Bucharest Romania

<sup>3</sup>University of Bucharest, Faculty of Physics, 405 Atomistilor street, 077125, Magurele, Romania

*Received July 30, 2013*

*Abstract.* The effect of DC reflex and RF plasma is observed on three types of wood samples: beech, oak and spruce. The aim is to perform surface hydrophilization and hydrophobization and characterize the modifications occurring at the surface of the wood. FTIR-ATR measurements were performed to characterize and identify the chemical bonds on the surface of the treated samples.

*Key words:* RF plasma, DC plasma, wood treatment, surface functionalization.

### 1. INTRODUCTION

Wood has been used for hundreds of thousands of years for both fuel and as a construction material, and is widely used in different industries. It is a renewable raw material, and can be found in different shapes and sizes all over the Earth. But wood, as a construction material, suffers in terms of durability, being susceptible to damage from insects, moisture and decay fungi. Currently, there are many available methods for wood treatment, to increase its durability, decrease its flammability, and increase the adherence of varnish and paint [1]. Many of these require high pressure – high temperature treatments involving dangerous chemicals, including pentachlorophenol (PCP), creosote, chromated copper arsenate (CCA), copper naphthenate, zinc naphthenate, or tributyltin oxide. The toxicity of the chemicals used in wood treatment has led to research into less toxic methods, like borates derived from boron (borax). Since borates are water soluble,

---

\* Paper presented at the 16<sup>th</sup> International Conference on Plasma Physics and Applications, June 20–25, 2013, Magurele, Bucharest, Romania.

they can be diluted and washed away in humid environments. Although the currently employed methods for treating wood have been proven over the past decades, there is a need for new, safe and environmentally friendly methods to increase the durability of wood, by enhancing the stability of water-based coatings and their adherence to the surface [2–4].

Over the past years, different plasma sources like RF, corona discharge, atmospheric or ionized jet, have been successfully used to enhance the properties of wood. Wood treatments in plasma ranges from increasing the adhesion properties of lignocellulosics [5, 6] to modifying the surface properties by hydrophilization [7–10] or hydrophobization [11, 12], and even decontamination [13] and fire-proofing [14].

Since the ban on Chromated Copper Arsenate, in 2003, and the restrictions on the use of creosotes, in 2013, the costs for wood treatments have increased dramatically, and plasma treatments seem to be a suitable competitor for environmental friendly technologies for improving wood properties.

The present paper, presents preliminary studies for surface modifications, which occur during the exposure of wood to RF and DC plasma. The goal of the experiments is to study the surface hydrophilization and hydrophobization by exposing different wood samples to plasma and study their effects on the surface. Contact angle (CA) measurements have been used to determine the effectiveness of the treatments by measuring the wettability of the surface of the wood. FTIR-ATR spectra have been used to study the modifications occurring in the cellulose, hemicellulose and lignin polymer chains which are present in the structure of the wood.

## 2. EXPERIMENTAL METHOD

Three types of Eastern European wood have been used for the study: beech (*Fagus sylvatica*), oak (*Quercus frainetto*) and spruce (*Picea abies*). For each wood type, samples were obtained from a 1 meter long heartwood plank, cut along the Longitudinal direction (*i.e.* along the wood fiber). The planks were not subjected to any chemical or heat treatments, and were used as obtained from the wood mill. From each plank, samples have been cut into pieces of 2 cm × 2 cm × 1 cm ( $W \times L \times H$ ) using a saw blade, as shown in Fig. 1. Control samples were cut from the same batches. CA measurements and FTIR-ATR spectra were performed on the samples before and after plasma exposure. For all samples, the characterized surface exposed to plasma was the LT plane.

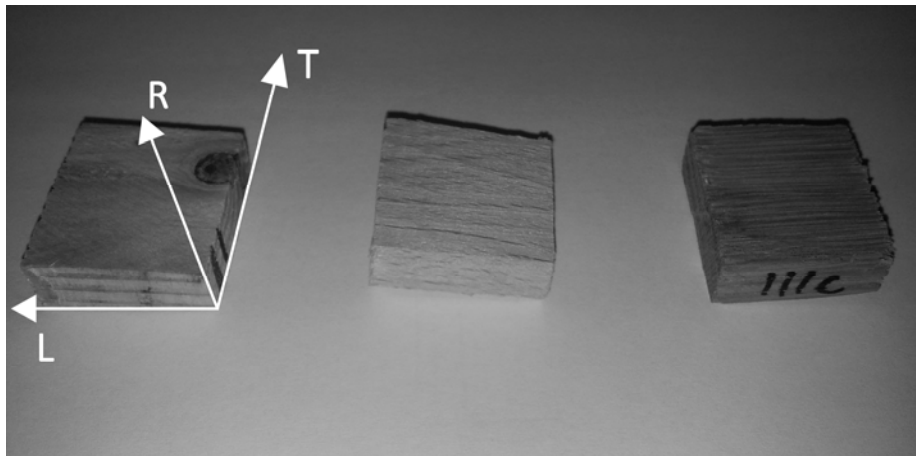


Fig. 1 – The image shows the spruce (left), beech (center) and oak (right) samples cut into 2 cm × 2cm × 1cm pieces (Longitudinal × Tangential × Radial directions). The characterized (upper) surface is the LT plane.

The RF plasma discharge studies are performed in a capacitive reactor (Sentech Instruments), using a 13.56 MHz radio frequency source. Argon gas plasma was used for hydrophilization experiments, while CHF<sub>3</sub> gas plasma was used for hydrophobization. The DC plasma discharge studies were performed in a custom built reactor using nitrogen gas. Tables 1 and 2 show the process parameters for RF and, respectively, DC reflex plasma experiments.

Table 1

Process parameters for RF plasma experiments

Process type	RF Power	Pressure	Gas flow	DC Bias	Time
Hydrophilization	20W	150 mTorr	Ar, 20 sccm	-90V	15 min
Hydrophobization	50W	300 mTorr	CHF <sub>3</sub> , 40 sccm	-65V	30 min

Table 2

Process parameters for DC reflex plasma experiments

Process type	DC Voltage	Current	Pressure	Gas flow	Time
Hydrophilization	505V	100mA	100 mTorr	N <sub>2</sub> , 100 sccm	30 min

The process parameters were tested on 3 samples of each wood type, to confirm sample to sample reproducibility. For each wood type, the samples were obtained from the same batch, as described earlier in the paragraph regarding sample preparation. Control samples for each wood type were exposed only to vacuum and process gas in order to separate the effects of the plasma treatment from other processing aspects such as exposure to low pressure during treatment, or exposure to the treatment gas.

The wood samples were analyzed by FTIR-ATR spectroscopy before and after plasma exposure in order to determine the changes occurring at the surface of the samples. The configuration of the chemical bonds was studied using a Tensor 27 Bruker Optics FTIR Spectrometer, using the ATR PIKE MIRacle with a single reflection ZnSe crystal. The spectra were plotted after 64 scans with a resolution of  $4\text{ cm}^{-1}$ , on a spectral range from  $4000\text{ cm}^{-1}$  to  $650\text{ cm}^{-1}$ . The static contact angle measurements were performed using an Attension Theta goniometer to determine the wettability of the samples.

### 3. RESULTS AND DISCUSSIONS

#### 3.1. WOOD HYDROPHILIZATION

After exposing the wood samples to Argon RF plasma, all the wood samples have shown a drastic decrease of the contact angle. During the measurements, the water droplet immediately spread over the surface of the wood, along the visible fibers, suggesting a highly hydrophilic behavior. Table 3 presents the contact angle measurements before and after RF plasma treatment.

*Table 3*

Contact angle measurements after RF Ar plasma

Sample	CA before treatment	CA after treatment
Beech	$26^\circ \pm 3^\circ$	N/A
Oak	$35^\circ \pm 3^\circ$	N/A
Spruce	$70^\circ \pm 3^\circ$	N/A

The control samples, exposed to vacuum and vacuum with Ar gas, have not shown any changes in wettability compared to the untreated samples, the contact angle being mostly the same, with a variation of  $\pm 3$  degrees. The variation of the CA for samples from the same batch may be due mostly to the surface roughness. The measurement was performed by placing a single droplet of water on each of the samples.

The samples were monitored for a period of 6 days, to verify the stability of the treatment. Between measurements, the samples were stored in clean room conditions, at  $21^\circ\text{C}$  and relative humidity  $\sim 30\%$ . The study shows the wood surfaces maintained the hydrophilic properties during this period. This kind of behavior is consistent with a chemical modification at the surface of the sample, which maintains a long term highly hydrophilic surface. During the contact angle measurements, the droplet does not seem to be absorbed into the volume of the sample, it only spreads over the surface.

For the DC plasma experiments, the wood samples were placed in the sheath of the DC reflex plasma reactor. After plasma exposure, the contact angle and the dynamic of the water droplet is visible modified, in comparison with the reference

sample. Table 4 presents the contact angle measurements before and after DC plasma treatment.

Table 4

Contact angle measurements after RF Ar plasma

Sample	CA before treatment	CA 24hrs after treatment	CA 72hrs after treatment
Beech	26° +/-3°	43° +/-3°	~11° +/-3°
Oak	35° +/-3°	~48° +/-3°	~16° +/-3°
Spruce	70° +/-3°	N/A	N/A

The control samples, exposed to vacuum and vacuum with N<sub>2</sub> gas, have not shown any changes in contact angle compared to the treated samples.

The samples were monitored over a three days period, and the contact angle has shown a wide dynamic over time. For all the tree samples, the contact angle of the reference is stable. After DC plasma treatment, for Beech and Oak the contact angle seems to increase at first, but the droplet is absorbed into the sample in a few minutes. Over the time of monitoring the samples, the contact angle decreases, and by the 3<sup>rd</sup> day, it stabilizes at 11°, for beech, and 16° for Oak. The measurements on the 3<sup>rd</sup> day have shown a stable contact angle, the droplet no longer being absorbed into the samples. For the Spruce, after the treatment, the droplet is absorbed very fast into the volume of the sample. In contrast, for the RF plasma treated samples the droplet does not seem to be absorbed, it only spreads over the surface.

Wood is mainly composed of polymer chains of cellulose, (Fig. 2), hemicellulose (Fig. 3), and lignin (Fig. 4), the quantity of each of the polymers being dependent on the type of wood.

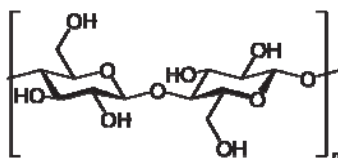


Fig. 2 – Cellulose chemical structure.

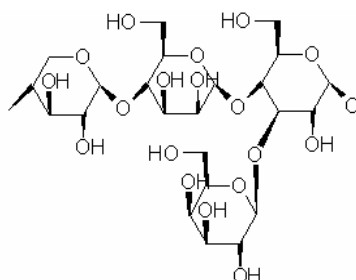


Fig. 3 – Hemicellulose chemical structure.

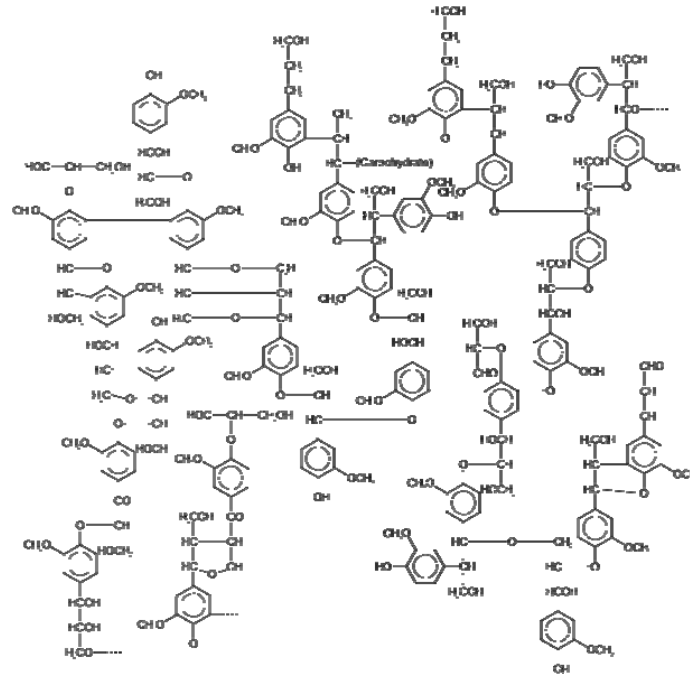


Fig. 4 – Lignin chemical structure [15].

FTIR-ATR analysis was performed to determine the chemical modifications of the polymer chains present at the surface of the wood.

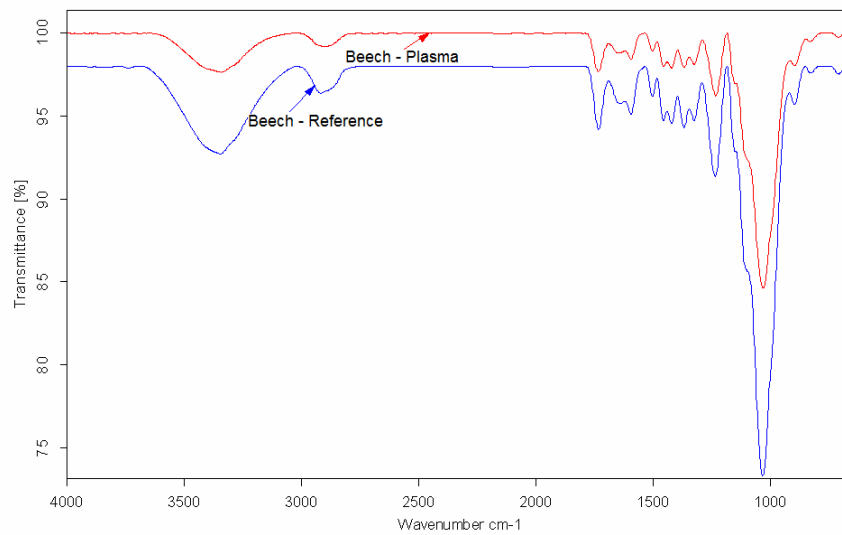


Fig. 5 – FTIR-ATR spectra of the beech tree sample before and after plasma treatment.

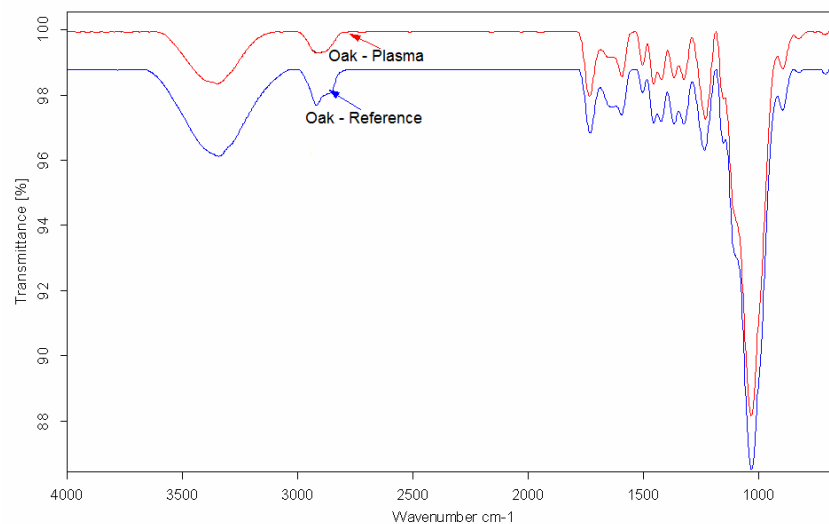


Fig. 6 – FTIR-ATR spectra of the oak tree sample before and after plasma treatment.

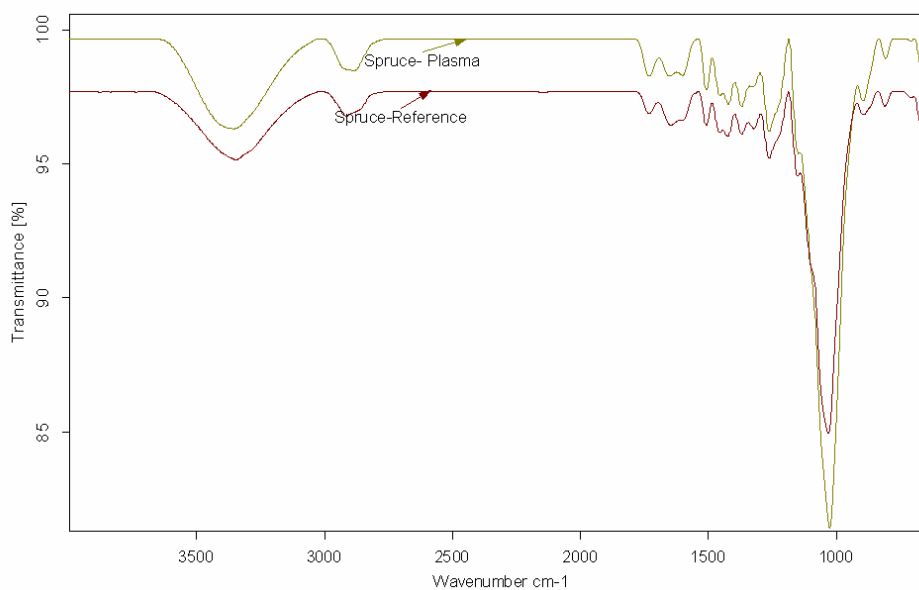


Fig. 7 – FTIR-ATR spectra of the spruce tree sample before and after plasma treatment.

The FTIR-ATR spectra shown in Figs. 5–7 were obtained for each sample before and after plasma exposure, thus a direct comparison of modifications occurring in the same sample being made. The spectra were obtained immediately before and after the exposure. Table 5 shows the identified peaks and their

respective attribution for each sample before and after plasma treatment.

For all of the studied wood samples, the 3500–2900  $\text{cm}^{-1}$  spectral range characterizes the vibration mode of the O-H bonds, with a maximum centered on 3300  $\text{cm}^{-1}$ , and the vibration mode of the C-H bonds, with a maximum centered around 2920  $\text{cm}^{-1}$ . We can consider the 1800–650  $\text{cm}^{-1}$  spectral range the fingerprint of the analyzed wood type, this region being characteristic to cellulose, hemicellulose, and lignin [16]. In the 1800–1500  $\text{cm}^{-1}$  spectral range we can observe the vibration modes of the unconjugated C = O bonds (1731–1735  $\text{cm}^{-1}$ ), while the 1645–1596  $\text{cm}^{-1}$  spectral bands can be attributed to the conjugated C-O bonds. The peaks at 1505  $\text{cm}^{-1}$  can be attributed to the C = C aromatic rings from the backbone of lignin. The 1800–1500  $\text{cm}^{-1}$  spectral range contains the bands characteristic to the vibration modes. The peaks in this range were assigned for the C-H bonds: 1457–1454  $\text{cm}^{-1}$  and 1424–1421  $\text{cm}^{-1}$  in lignin, 1370–1368  $\text{cm}^{-1}$  in cellulose and hemicellulose, 1327–1323  $\text{cm}^{-1}$  in cellulose [17, 18]. The pyranose ring and the aromatic ring from the cellulose backbone are shown by the vibration mode of the C-O bond at 1030  $\text{cm}^{-1}$  and 1230  $\text{cm}^{-1}$ , respectively. The peaks at 890  $\text{cm}^{-1}$  and 660  $\text{cm}^{-1}$ , appear due to the vibration mode of the C-H bonds in cellulose and lignin [19–21].

Table 5

FTIR peaks identification and attribution for treated and untreated samples

Wavenumber ( $\text{cm}^{-1}$ )						Peak attribution
Beech		Oak		Spruce		
Ref.	Ar treated	Ref.	Ar treated	Ref.	Ar treated	
3346	3341			3345	3353	O-H
2917	2903	2918	2912	2915	2885	C-H
1734	1735	1733	1735	1731	1731	C=O
1641	1649	1649	1656	1646	1652	C-O, O-H
1596	1596	1596	1595	1596	1601	C-O, aromatic ring
1505	1504	1505	1505	1508	1507	Aromatic ring
1457	1456	1457	1457	1454	1454	C-H
1422	1423	1424	1423	1424	1421	C-H
1370	1369	1368	1368	1369	1369	C-H
1326	1326	1325	1326	1323	1327	C-H
1237	1234	1236	1233	1262	1262	Aromatic ring
1034	1032	1032	1034	1030	1025	C-O
899	899	898	897	893	895	C-H
663	663	661	663	664	660	C-H

The comparison between the treated and untreated samples shows that the characteristic absorption bands are in the same spectral domains. Slight differences appear in the intensity and shifting of the bands characteristic to the vibration mode of the analyzed samples. For the plasma treated samples, the spectral bands associated to C-H aliphatic groups suffer a slight decrease in intensity, while the

carbonyl group shows an increase in intensity and a shift towards lower wavenumbers compared to the reference, which suggests a mild oxidation of the wood surface [22]. Importantly, we did not observe the disappearance or additional formation of any bond after the plasma exposure. The bonds found in the reference measurement are slightly shifted, as shown in Table 5, and show different intensities, as shown in Figs. 5–7.

The hydrophilization of the surface should be a result of the interaction between the plasma species and the surface of the samples. For the RF plasma experiments, the samples were placed in the sheath on the lower electrode. During plasma exposure, the lower electrode is self-biased at a negative potential, as shown in Table 1, which attracts the positively charged ions. Due to the limited data obtained from the FTIR-ATR measurements, we can only assume that during exposure to inert gas plasmas, the covalent bonds in the amorphous polymer chains are broken, thus creating free radicals at the surface of wood. When the samples are exposed to the atmosphere, the plasma activated surface readily adsorbs the moisture that is present in the environment. The exposure of the wood to the inert gas plasma is sufficient to abstract hydrogen or oxygen and to form free radicals at or near the surface, which then interact to form the cross-links and unsaturated groups with the chain scission. The plasma also removes the low molecular-weight materials, such as the side groups on the chain molecules or amorphous cellulose and hemicellulose, or converts them to a higher molecular weight by cross-linking reactions [23, 24]. This effect could be in accordance with the slight oxidation of the surface, indicated by the shifting of the aromatic rings and aliphatic C-H groups. This treatment has been known as CASING (cross-linkage by activated species of inert gases) [25, 26], and the effect is consistent with the long term stability of the contact angle of our samples, the hydroxyl groups forming strong bonds with the aromatic rings present in the polymer backbones.

For the DC plasma, the samples are placed in the plasma sheath. The lower energy of the species present in this region is not sufficient to break chemical bonds at the surface of the polymer chains. For this case, the FTIR-ATR spectra were quite similar to the untreated samples. Similar to the RF plasma case, the characteristic absorption bands are in the same spectral domains. Slight but inconclusive differences appear in the intensity of the vibration mode of the analyzed samples.

FTIR-ATR analysis alone, can offer only a qualitative measurement, not a quantitative one, thus it is not enough to emphasize the modifications occurring at the surface of the wood samples.

### 3.2. WOOD HYDROPHOBIZATION

After exposing the wood samples to CHF<sub>3</sub> RF plasma, all the wood samples have shown a drastic increase of the contact angle, the surface becoming highly hydrophobic. Table 6 presents the contact angle measurements before and after RF plasma treatment, as well as the time evolution of the droplet.

Table 6

Beech tree hydrophobization, evolution of the contact angle over 6 days

CA before treatment	CA after treatment					
	0h	24h	48h	72h	96h	144h
~26°	~145°	~137°	~129°	~122°	~115°	~115°

The samples were monitored for a period of 6 days, to check the stability of the treatment. The study shows the wood surfaces maintained hydrophobic during this period. Immediately after the treatment, the contact angle increased to ~145°. The following days, it slowly decreased to ~115°, and it stabilized for the remainder of the monitoring period. Each day, several measurements were performed on each of the three samples. After each measurement the water droplet was blown away using a nitrogen gun. Measurements on the same sample show the same contact angle, while sample to sample comparison show a variation of  $\pm 1^\circ$ .

The modification of the contact angle is due to the deposition of a fluoropolymer on the surface of the wood, confirmed by FTIR-ATR analysis (Fig. 8).

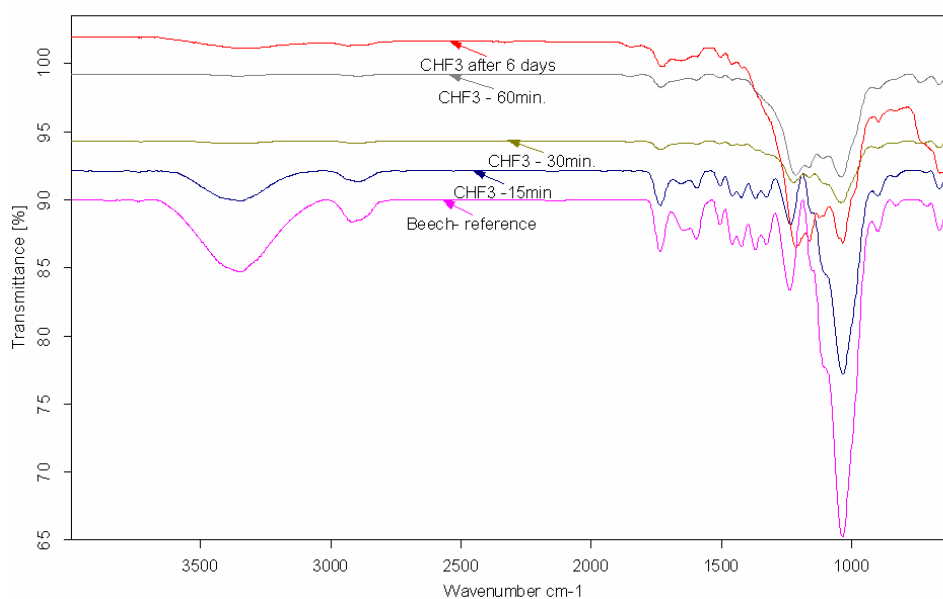


Fig. 8 – FTIR-ATR spectra of the beech tree sample. “CHF3-15min” is the sample treated for 15 minutes, “CHF3-30min” is the sample treated for 30 minutes, “CHF3-60min” is the sample treated for 60 minutes, while “CHF3 after 6 days” is the sample treated for 60 minutes 6 days after the plasma treatment.

As the treatment time is increased, the intensity of the vibration mode of the O-H groups and C-H aliphatic groups decreases. After 30 minutes, the vibration

modes in the 3500–2900  $\text{cm}^{-1}$  spectral range completely disappear, while in the spectral range between 1200–1100  $\text{cm}^{-1}$  a valence vibration bond appears, and a deformation vibration is visible at 735  $\text{cm}^{-1}$ . These vibrations belong to the C-F bond. The deformation vibrations of the C-H bond disappear from the 1300–1450  $\text{cm}^{-1}$  spectral range. The appearance of new C-F bonds confirms the deposition of the fluoropolymer layer. The disappearance of C-H vibration modes, suggest the replacement of O-H and C-H bonds from the polymer backbone.

After monitoring the contact angle for 6 days, another FTIR-ATR measurement was performed on the sample. The measurements, as seen in Fig. 8, show the slight appearance of O-H and C-H bonds in the 3500–2900  $\text{cm}^{-1}$  spectral range after a few days monitoring. This might be due to the continuous interaction of the deposited fluoropolymer with the moisture in the atmosphere and the water used for contact angle measurements. None the less, the contact angle measurements still reveal a highly hydrophobic surface.

#### 4. CONCLUSIONS

We have successfully hydrophilized the surface of the wood by inert gas plasma. The FTIR-ATR measurements could not provide sufficient information in order to confirm the modifications observed on the surface. The conclusions were based by comparison with papers describing the plasma treatment of other polymers, in our opinion the mechanism of interaction being largely the same. The modified hydrophilic surfaces were stable over the monitoring period, suggesting a permanent bond between hydroxyl absorbed from the atmosphere and the polymer backbone. The results obtained on DC reflex plasma are similar to those presented in the available literature [5–10], while the RF plasma discharge shows a much smaller contact angle. Even though the CA obtained by the RF Argon plasma is better, further experiments are required to prove the method's efficiency in improving the adhesion of protective coatings.

The hydrophobization of the surface was performed by deposition of a Teflon-like fluoropolymer, resulting in a highly stable hydrophobic surface. FTIR-ATR measurements confirmed the deposition of the polymer, and the inhibition of moisture exchange between the wood sample and water. The modified hydrophobic surfaces were relatively stable over the monitoring period. The obtained results are similar to those presented in literature, the novelty of our method stands in the use of trifluoromethane as process gas, compared to fluorine rich gasses [27, 28] or surface silylation [5, 11, 29] presented in the literature.

#### REFERENCES

1. B.A. Richardson, *Lancaster a.o.*, The Construction Press, 1978.
2. K. Tsunoda, *J. Wood Sci.*, **47**, 2, 2001.
3. M. Muin, K. Tsunoda, *J. Wood Sci.*, **49**, 5 (2003).

4. S. Nami Karta, *Holzforschung*, **60**, 4 (2006).
5. R. Mahlberg, H. E.-M. Niemi, F. Denes, R.M. Rowell, *Int. J. Adhes. Adhes.*, **18**, (1998).
6. M.N. Acda, E.E. Devera, R.J. Cabangon, H.J. Ramos, *Int. J. Adhes. Adhes.*, **32** (2012).
7. L. Podgorski, B. Chevet, L. Onic, A. Merlin, *Int. J. Adhes. Adhes.*, **20**, 2 (2000).
8. P. Rehn, W. Viöl, *Holz Roh Werkst.*, **61**, 2 (2003).
9. M. Odrášková, J. Ráhel', A. Zahoranová, R. Tiño, M. Černák, *Plasma Chem. Plasma P.*, **28**, 2 (2009).
10. E. Gătin, D. Alexandreanu, C. Berlic, A. Popescu, E. Barna, D. Moja, *Physica Medica*, **XVI**, 1, 3 (2000).
11. P. Rehn, A. Wolkenhauer, M. Bente, S. Förster, W. Viöl, *Surf. Coat Tech.*, 174–175 (2003).
12. M. Bente, G. Avramidis, S. Förster, E.G. Rohwer, W. Viöl, *Holz Roh Werkst.*, **62**, 3 (2004).
13. C. Leclaire, E. Lecoq, G. Oriol, F. Clement, F. Boust, COST Action IE0601, November 5–7<sup>th</sup>, 2008, Braga, Portugal.
14. K.G. Pabeliña, C.O. Lumban, H.J. Ramos, *Nucl. Instrum. Meth. B*, **272** (2012).
15. A. W. Glazer and H. Nikaido, *Microbial Biotechnology: fundamentals of applied microbiology*, San Francisco: W. H. Freeman, 1995, p. 340.
16. M.A. Tshabalala, J. Jakes, M.R. Van Ledingham, S. Wang, J. Peltonen, *Handbook of Wood Chemistry and Wood Composites, Second Edition*, Roger M. Rowell, CRC Press, 2012.
17. G. Müller, C. Schöpfer, H. Vos, A. Kharazipour, A. Poll, *BioResources*, **4**, 1, 49–71 (2009).
18. M. C. Timar, A.A. Tuduce Trastaru, S. Patachia, C. Croitoru, *Proligno*, **7**, 1, 25–38 (2011)
19. H. Yang, R. Yan, H. Chen, D.H. Lee, C. Zheng, *Fuel*, **86** (2007).
20. A. Emandi, C. Vasiliu, P. Budrugaec, I. Stamatina, *Cell. Chem. Technol.*, **45**, 9–10 (2011).
21. G. Socrates, *Infrared and Raman Characteristic Group Frequencies*, Wiley, John & Sons, Incorporated, 2004.
22. C. Lux, Z. Szalay, W. Beikircher, D. Kovacik, H. Pulker, *Eur. J. Wood Prod.*, **71**, 539–549 (2013).
23. S. Guruvenket, G.M. Rao, M. Komath, A.M. Raichur, *Appl. Surf. Sci.*, **236**, 1–4 (2004).
24. R.M. France, R.D. Short, *Langmuir*, **14**, 17 (1998).
25. R.H. Hansen, H. Schonhorn, *J. Poly. Sci., B*, **4**, 203 (1966).
26. H. Schonhorn, R.H. Hansen, *J. Appl. Poly. Sci.*, **11**, 1461 (1967).
27. F. Denes, Z.Q. Hua, *J. Appl. Polym. Sci.*, **71**, 1627–1639 (1999).
28. A.R. Denes, M. Tsabalala, R. Rowell, F. Denes, and R.A. Young, *Holzforschung*, **53**, 318–326 (1999).
29. M. Andresen, L.S. Johansson, B.S. Tanem, P. Stenius, *Cellulose*, **13**, 665–667 (2006).